

# Gamma-Ray emission from CCO 1E 1207.4-5209 and its host SNR G296.5+10.0

Luana N. Padilha,<sup>a,1</sup> Rita C. dos Anjos,<sup>a,b,c</sup> Jaziel G. Coelho<sup>d,e</sup>

<sup>a</sup>Programa de pós-graduação em Física & Departamento de Física, Universidade Estadual de Londrina (UEL), 86057-970 Londrina, PR, Brazil

<sup>b</sup>Departamento de Engenharias e Exatas, Universidade Federal do Paraná (UFPR), Pioneiro, 2153, 85950-000 Palotina, PR, Brazil

<sup>c</sup>Applied Physics Graduation Program, Federal University of Latin-American Integration, 85867-670, Foz do Iguaçu, PR, Brazil

<sup>d</sup>Núcleo de Astrofísica e Cosmologia (Cosmo-Ufes) & Departamento de Física, Universidade Federal do Espírito Santo, 29075-910, Vitória, ES, Brazil

<sup>e</sup>Divisão de Astrofísica, Instituto Nacional de Pesquisas Espaciais, Avenida dos Astronautas 1758, 12227-010, São José dos Campos, SP, Brazil

E-mail: [luana.natalie.padilha@uel.br](mailto:luana.natalie.padilha@uel.br), [ritacassia@ufpr.br](mailto:ritacassia@ufpr.br), [jaziel.coelho@ufes.br](mailto:jaziel.coelho@ufes.br)

**Abstract.** The origin and acceleration mechanisms of energetic particles in the universe remain enigmatic in contemporary astrophysics. Recent efforts have focused on identifying Galactic sources capable of accelerating particles to 1 PeV, known as PeVatrons. The different morphology of galactic supernova remnants is directly related to the type of stellar explosion and the existence of a possible Compact Central Object (CCO), which possess intense radiative-gravitational fields on their surfaces. These CCOs, due to their strong fields and interactions with surrounding magnetic clouds, are potential candidates for cosmic ray production. Through observations of the compact X-ray source 1E 1207.4-5209, located near the remnant G296.5+10.0, and using the enhanced GALPROP code, we analyze the emission of high-energy gamma rays ( $E > 100$  GeV) resulting from cosmic-ray acceleration and propagation. Additionally, we calculate the contribution of this association to the overall observed Galactic cosmic-ray flux, considering cosmic-ray propagation within the Galaxy, including energy losses and particle interactions. Our findings suggest that this setup offers a fertile environment for the production of a wide range of cosmic-ray energies, ranging from GeV to TeV, and even extending up to PeV, within the Galaxy.

---

<sup>1</sup>Corresponding author.

---

## Contents

<b>1</b>	<b>Introduction</b>	<b>1</b>
<b>2</b>	<b>CCO 1E 1207.4-5209 and its host SNR G296.5 + 10.0</b>	<b>2</b>
<b>3</b>	<b>Description of simulation models</b>	<b>2</b>
<b>4</b>	<b>Discussions</b>	<b>4</b>
<b>5</b>	<b>Summary</b>	<b>4</b>

---

## 1 Introduction

Extensive research has revealed that many astrophysical objects within our galaxy are, in fact, neutron stars (NS). Intriguingly, these discoveries often align with the locations of Supernova Remnants (SNRs) [1]. These sources, known as Compact Central Objects (CCOs), are identifiable by their intense thermal X-ray emissions and a notable absence of radio and gamma-ray emissions [2]. In particular, CCOs exhibit characteristics [see 3, 4] that make them ideal candidates for particle acceleration to extremely high energies. This potential is amplified by the fact that CCOs and their associated supernova remnants provide an excellent opportunity to integrate kinematic data from both the neutron star and the supernova shock wave [1].

Supernova remnants and the potential presence of CCOs are inherently linked to the type of explosion of the progenitor star. Consequently, they exhibit distinct morphologies, often influenced by the materials in their vicinity and the compression of diverse magnetic fields [5]. CCOs are astronomical entities located at the geometric centers of supernova remnants, characterized by thermal X-ray emissions in the hundreds of electronvolts (eV) range and luminosities ranging from  $10^{33}$  to  $10^{34}$  (erg/s<sup>-1</sup>) [see, e.g., 6, 7]. An intriguing characteristic of these objects is their minimal emissions in alternative energy bands [2, 7, 8]. Due to their elusive nature, only ten CCOs have been officially cataloged, with many more potentially existing but not yet discovered [see, e.g., 1]. Measurements of their rotational periods and decay rates indicate that these objects possess antimagnetic properties, with weak magnetic fields spanning the range of  $10^{10}$  to  $10^{11}$  G. These weak magnetic fields likely stem from magnetic dipole braking, suggesting that CCOs are relatively young entities [see, e.g., 9].

Multimessenger astronomy approaches to the origin search of cosmic rays (CRs) are based on the inclusion of all available information from charged CRs and neutral secondaries generated near sources by interactions. In particular, neutron and gamma rays flux through the interaction of CRs with fields. Furthermore, accelerated electrons and positrons can produce radiation through the synchrotron emission, bremsstrahlung and Inverse Compton [10, 11]. The relationship between the propagation of cosmic rays and the integral flux of secondary gamma-rays from a source determined cosmic ray luminosities in models both inside and outside of our Galaxy [12–16].

This paper calculates the contribution of the secondary gamma rays from charge particles by the CCO 1E 1207.4-5209 and its host SNR G296.5 + 10.0 association using the

v57 GALPROP release [17] with 3D maps of the Galactic magnetic field, diffuse interstellar medium (ISM) distributions, the interstellar radiation field (ISRF), and the gas distribution throughout the Galaxy. This manuscript is organized as follows. The next section presents in detail the association CCO 1E 1207.4-5209 and its host SNR G296.5 + 10.0. The third section presents the description of simulation models. Beyond that, in this section we describe our multimessenger analysis. The final section provides the primary concluding observations and discussions of this investigation.

## 2 CCO 1E 1207.4-5209 and its host SNR G296.5 + 10.0

The neutron star 1E 1207.4-5209 is a quiet, fast-rotating object of the CCO class [18]. Situated at the geometric center of the supernova remnant G296.5+10.0 (also named PKS 1209-51), the CCO 1E 1207.4-5209 was the focus of a comprehensive XMM-Newton spacecraft observation in August 2002 [19]. Using the EPIC 12,13 instrument, the observations lasted approximately 36 hours and significantly advanced the study of its emission [20]. This compact central object (CCO) possesses a rotational period of 0.42413076 seconds, and its period derivative is constrained by an upper limit of  $2.224 \times 10^{-17} \text{ s}; \text{s}^{-1}$  (according to the ATNF catalog<sup>1</sup>). Situated in the Centaurus constellation, it is positioned at a distance of 2 kiloparsecs [21]. As reported by [20], the light curve of this object spans an energy range from 0.2 to 4 keV.

The supernova remnant G296.5+10.0 exhibits intense X-ray and radio emissions concentrated in the southern, eastern, and southwestern regions [22]. It possesses a bilateral morphology, with symmetry axes parallel to the Galactic plane and two bright arms on the sides. Some experts suggest that the remnant features tangentially positioned filaments composed of compressed cold gas clouds [see 23], along with a shell consisting of  $H_I$  [24].

This source stands out as a unique computational neutron star in which the magnetic field is directly measured, rather than being inferred as in other objects of its class. The XMM-Newton telescope detected X-ray absorption lines in its spectrum, which can be interpreted as cyclotron resonance of electrons near the central object’s surface. The cyclotron lines (0.7 keV) correspond to a magnetic field of approximately  $8 \times 10^{10} \text{ G}$  or  $1.6 \times 10^{14} \text{ G}$  [see 9, 20, 25, 26]. Another intriguing characteristic of this CCO is its age, as it is believed to have formed simultaneously with the associated supernova remnant, given its origin linked to the death of the progenitor star. However, the remarkable age of 1E 1207.4-5209 exceeds by three orders of magnitude the age of the supernova G296.5+10.0. This suggests the presence of a significant braking index, especially if the current rotation period of the star is approximated to its characteristic period [see, e.g., 25]. These features make this CCO notable among other known pulsars.

## 3 Description of simulation models

In its most recent version 57, the GALPROP program was utilized to create a realistic model. GALPROP solves the transport equation for a given source distribution while accounting for all spatial and energetic processes that the particles encounter during propagation [17]. The transport equation is solved by the software using the Crank-Nicholson model of second order. Utilizing source abundance relations for isotope generation and the boron-carbon ratio in terms of the stiffness and dispersion characteristics, the diffusion coefficient is computed

<sup>1</sup><https://www.atnf.csiro.au/research/pulsar/psrcat/>; Pulsar name: J1210-5226

[see 16, for details]. The Galactic gas distribution was modeled using a high column density  $H$  model [27]. Energy losses from synchrotron and Compton scattering processes are taken into account by the GALPROP code, which calculates the losses using an observer centered on the solar system. Furthermore, the interstellar radiation field is modeled using an R12 model [see 28]. For the magnetic field, a basic exponential model is taken into consideration [see 29, for details]. An overview of the simulation parameters is provided in Table 1.

**Table 1:** Simulation parameters

Parameters	Values	Units
Grid	$\begin{cases} x & -18.0 : +18.0 \\ y & -18.0 : +18.0 \\ z & -4.0 : +4.0 \end{cases}$	kpc
$E_{min}$	1	MeV
$E_{max}$	$1.0 \times 10^{11}$	MeV
$D_{0,xx}$	$2.5 \times 10^{28}$	$\text{cm}^2 \text{s}^{-1}$
$V_a$	28.0	$\text{km s}^{-1}$

Several models that consider different particle injection models can be performed using the software. In our model, we use a differential injection spectrum that adheres to a momentum power law distribution, characterized by indices of 2.2 - 2.4 [30, 31]. The spin-down model was the first emission model to be taken into account. According to this scenario, dipole radiation is the reason why the pulsar is losing power. With an injection power that follows a power law with a smooth break and accelerated acceleration, the model implies that the spectrum is normalized by [16, 17, 32, 33]

$$L(t) = \eta L_0 \left( 1 + \frac{t}{\tau_0} \right)^{-2}, \quad (3.1)$$

where  $L_0 = 1.0 \times 10^{33} \text{ erg s}^{-1}$  is the initial rotational power of the source,  $\eta = 1$  is the efficiency, and  $\tau_0 = 3.63 \times 10^5 \text{ yr}$  is the time scale of the pulsar. The rate of cosmic-ray production correlates with the spin down of pulsars [see 16, 33].

The second model used quiescent emission or magnetic energy injection to produce a cosmic ray luminosity  $L'$  and, in turn, a gamma-ray luminosity derived from the upper limits of the H.E.S.S. Collaboration [34]. Assuming a spectral index of  $E^{-1.9}$ , the integral upper limits obtained from H.E.S.S. observation can be converted into upper limits on the flux  $F(1 \text{ GeV} < E < 1 \text{ TeV})$  is the  $(1.19 \pm 0.11) \times 10^{-9} \text{ cm}^{-2} \text{s}^{-1}$  at 99.5% CL [35]. The secondary gamma-ray flux generated by SNR G296.5 + 10.0 is proportional to its cosmic-ray flux or luminosity, according to the model described in [15, 16]. Consequently, the gamma-ray generation rate per unit volume may be expressed as a function of cosmic-ray luminosity and is conservative. Therefore, the total luminosity ( $L$ ) of the association source is given by the sum of spin-down and quiescent emissions ( $L = L(t) + L'$ ).

The results derived for the gamma-ray emission and spectral energy distribution from these models are discussed in the following section. Simulations are based on the parameters of the association CCO 1E 1207.4-5209 + SNR G296.5 + 10.0.

## 4 Discussions

This section contains the results of the transport models we developed. We begin by analyzing the spectra distributions of four elements in cosmic rays using distinct model emission. The 2D gas distribution of interstellar gas was used to simulate the models [28, 36]. Figure 1 shows the spectral energy distribution of the gamma-ray emissions resulting from the proton in CCO 1E 1207.4-5209 and its associated Supernova Remnant (SNR) G296.5 + 10.0 to the spectral index 2.2 - (a), 2.4 - (b) and 2.6 - (c). A range of values between 2.0 and 2.6 was selected according to the spectrum of individual sources and observations as described in [15, 30].

The spin-down model is a more effective injection model since it shows a higher particle flux in Fig. 1 compared to the quiescent model. Consequently, it may be inferred that the rotating properties of the object lead to a higher particle injection power. The plot illustrates the poor gamma-ray data/model of CCO 1E 1207.4-5209 and its corresponding Supernova Remnant (SNR) G296.5 + 10.0. This is based on the model proposed by [35] and the gamma ray measurements conducted by [37]. The lines indicate a larger fraction of gamma radiation emission in the energy range of  $10^2 - 10^5$  MeV, where the simulation data meets the CCO gamma emission data [37], for all spectral index Fig. 1-(a,b,c). In the spin-down scenario, gamma-ray emission is mostly produced by pion decay. Specifically, in Fig. 1-(a) at the VHE spectrum and at lower energy in Fig. 1-(b,c).

Figures 2 and 3 show the energy spectra for proton and other elements, respectively. The Fig. 2 describes how the source contributes to the overall proton cosmic ray flux, considering three different spectral indices: 2.2 (see Fig. 2 - (a)), 2.4 (see Fig. 2 - (b)), and 2.6 (see Fig. 2 - (c)). The spin-down model accounts for most of the spectrum, and a spectral index of 2.2 provides the best description of the data at the highest energy levels. The spectra demonstrated in Fig. 3 follow a pattern similar to that in Fig. 2. However, as expected, the impact of the source on the spectra of heavier elements is significantly diminished as a result of the reduced flux of these particles. The presence of a CCO associated with a supernova event may promote the emission of charged and multi-messenger particles.

The B/C ratio against kinetic energy per nucleon for our models in comparison with CR data is shown in Fig. 4. Since there is only one point source, the purpose of this illustration was not to elucidate the data. Instead, its objective was to establish a comparison between the contributions of the emission models. Moreover, it becomes apparent that the spin-down contribution is effective in explaining the data. Finally, we investigate the impact of the gas distribution on the total predicted gamma-ray intensity for the spin-down model in Figure 5. The impact of alternate gas maps on the spectrum is discussed in detail in [31]. The figures depict the intensity calculated at both 1 GeV and 1 TeV for electron emissions through inverse Compton and bremsstrahlung processes, utilizing the 3D gas model. The three-dimensional spatial density model for neutral and molecular hydrogen was developed based on gas line-survey data [27]. There is an increase in intensity at 1 TeV for both inverse Compton and bremsstrahlung processes.

## 5 Summary

In this study, we generated gamma-ray spectra from cosmic rays through simulations involving the association of the only pulsar with an inferred magnetic field, CCO 1E 1207.4-5209, and the supernova remnant G296.5 + 10.0. We considered three different emission scenarios

at the source. Our findings are a direct result of energy particle propagation processes up to  $10^{14}$  eV, emphasizing the need to construct and assess propagation models to understand the physics of Galactic cosmic rays and the emission zone of PeVatrons inside our Galaxy. The spin-down model contributed the most to our findings, highlighting the potential of this association in contributing to various multi-messenger emissions within the Galaxy. Nevertheless the limited availability of source emission data prevents us from making more extensive conclusions. Moving forward, the utilization of Cherenkov Telescope Array (CTA) measurements [see 38] will yield enhanced understanding and prospects for modeling the emissions emitted by this CCO and other sources of low-gamma emission.

## Acknowledgments

This study was financed in part by the Coordenação de Aperfeiçoamento de Pessoal de Nível Superior – Brasil (CAPES) – Finance Code 001. J.G.C. is grateful for the support of FAPES (1020/2022, 1081/2022, 976/2022, 332/2023) and CNPq (311758/2021-5). The research of R.C.A. is supported by Conselho Nacional de Desenvolvimento Científico e Tecnológico (CNPq), grant number 310448/2021-2. R.C.A. and L.N.P are grateful for the support of L’Oreal Brazil, with partnership of ABC and UNESCO in Brazil. The authors acknowledge the National Laboratory for Scientific Computing (LNCC/MCTI, Brazil) for providing HPC resources of the SDumont supercomputer, which have contributed to the research results reported in this paper. URL: <http://sdumont.lncc.br>. J.G.C and R.C.A acknowledge the financial support of FAPESP Project No. 2021/01089-1. The authors acknowledge the financial support of NAPI *Fenômenos Extremos do Universo* of Fundação de Apoio a Ciência, Tecnologia e Inovação do Paraná.

## References

- [1] M.G.F. Mayer and W. Becker, *A kinematic study of central compact objects and their host supernova remnants*, *A&A* **651** (2021) A40 [2106.00700].
- [2] A.K. Harding, *The neutron star zoo*, *Frontiers of Physics* **8** (2013) 679 [1302.0869].
- [3] A.M. Hillas, *Where do  $10^{19}$  eV cosmic rays come from?*, *Nuclear Physics B Proceedings Supplements* **136** (2004) 139.
- [4] K.V. Ptitsyna and S.V. Troitsky, *Physical conditions in potential accelerators of ultra-high-energy cosmic rays: updated Hillas plot and radiation-loss constraints*, *Physics Uspekhi* **53** (2010) 691 [0808.0367].
- [5] L.A. Lopez and R.A. Fesen, *The Morphologies and Kinematics of Supernova Remnants*, *Space Science Reviews* **214** (2018) 44 [1804.00024].
- [6] J.P. Halpern and E.V. Gotthelf, *Spin-Down Measurement of PSR J1852+0040 in Kesteven 79: Central Compact Objects as Anti-Magnetars*, *ApJ* **709** (2010) 436 [0911.0093].
- [7] G.G. Pavlov, D. Sanwal and M.A. Teter, *Central Compact Objects in Supernova Remnants*, in *Young Neutron Stars and Their Environments*, F. Camilo and B.M. Gaensler, eds., vol. 218, p. 239, Jan., 2004, DOI [astro-ph/0311526].
- [8] A. De Luca, *Central compact objects in supernova remnants*, in *Journal of Physics Conference Series*, vol. 932 of *Journal of Physics Conference Series*, p. 012006, Dec., 2017, DOI [1711.07210].
- [9] J.P. Halpern and E.V. Gotthelf, *Spin-Down Measurement of PSR J1852+0040 in Kesteven 79: Central Compact Objects as Anti-Magnetars*, *ApJ* **709** (2010) 436 [0911.0093].

- [10] J. Becker Tjus, *Search for Galactic cosmic ray sources: The multimessenger approach*, in *European Physical Journal Web of Conferences*, vol. 105 of *European Physical Journal Web of Conferences*, p. 00003, Dec., 2015, DOI.
- [11] J. Becker Tjus and L. Merten, *Closing in on the origin of Galactic cosmic rays using multimessenger information*, *Physics Reports* **872** (2020) 1 [2002.00964].
- [12] A.D. Supanitsky and V. de Souza, *An upper limit on the cosmic-ray luminosity of individual sources from gamma-ray observations*, *JCAP* **2013** (2013) 023 [1311.4820].
- [13] R.C. Anjos, V. de Souza and A.D. Supanitsky, *Upper limits on the total cosmic-ray luminosity of individual sources*, *JCAP* **2014** (2014) 049 [1405.3937].
- [14] R. Sasse and R.C. dos Anjos, *Upper limits on the cosmic-ray luminosity of supernovae in nearby galaxies*, in *37th International Cosmic Ray Conference*, p. 461, Mar., 2022, DOI.
- [15] R.C. dos Anjos, J.G. Coelho, J.P. Pereira and F. Catalani, *High-energy gamma-ray emission from SNR G57.2+0.8 hosting SGR J1935+2154*, *JCAP* **2021** (2021) 023 [2106.03008].
- [16] J.G. Coelho, L.N. Padilha, R.C. dos Anjos, C.V. Ventura and G.A. Carvalho, *An updated view and perspectives on high-energy gamma-ray emission from SGR J1935+2154 and its environment*, *JCAP* **2022** (2022) 041 [2204.09734].
- [17] T.A. Porter, G. Jóhannesson and I.V. Moskalenko, *The GALPROP Cosmic-ray Propagation and Nonthermal Emissions Framework: Release v57*, *ApJS* **262** (2022) 30 [2112.12745].
- [18] B. Gong, *Radio-quiet neutron star 1E 1207.4-5209 : a possible strong gravitational-wave source.*, *PRL* **95** (2005) 1101 [astro-ph/0506431].
- [19] S. Mereghetti, A. De Luca, P.A. Caraveo, W. Becker, R. Mignani and G.F. Bignami, *Pulse Phase Variations of the X-Ray Spectral Features in the Radio-quiet Neutron Star 1E 1207-5209*, *ApJ* **581** (2002) 1280 [astro-ph/0207296].
- [20] A. De Luca, S. Mereghetti, P.A. Caraveo, M. Moroni, R.P. Mignani and G.F. Bignami, *XMM-Newton and VLT observations of the isolated neutron star 1E 1207.4-5209*, *A&A* **418** (2004) 625 [astro-ph/0312646].
- [21] V.E. Zavlin, G.G. Pavlov, D. Sanwal and J. Trümper, *Discovery of 424 Millisecond Pulsations from the Radio-quiet Neutron Star in the Supernova Remnant PKS 1209-51/52*, *ApJL* **540** (2000) L25 [astro-ph/0005548].
- [22] A. Moranchel-Basurto, P.F. Velázquez, E. Giacani, J.C. Toledo-Roy, E.M. Schneiter, F. De Colle et al., *Origin of the bilateral structure of the supernova remnant G296.5+10*, *MNRAS* **472** (2017) 2117 [1709.00460].
- [23] R.S. Roger, D.K. Milne, M.J. Kesteven, K.J. Wellington and R.F. Haynes, *Symmetry of the Radio Emission from Two High-Latitude Supernova Remnants, G296.5+10.0 and G324.7+14.6 (SN 1006)*, *ApJ* **332** (1988) 940.
- [24] G.M. Dubner, F.R. Colomb and E.B. Giacani, *1410 MHz continuum and HI line observations towards the SNR G 296.5+10.0 and nearby sources. Evidences of two SNRs tunneling through the interstellar medium.*, *Astronomical Journal* **91** (1986) 343.
- [25] A. Ankey, A.M. Ankey and E.N. Ercan, *Possible Evolution of DIM Radio-Quiet Neutron Star 1e 1207.4-5209 Based on a B-Decay Model*, *International Journal of Modern Physics D* **16** (2007) 619 [0706.0831].
- [26] G.G. Pavlov and V.G. Bezchastnov, *Once-ionized Helium in Superstrong Magnetic Fields*, *ApJL* **635** (2005) L61 [astro-ph/0505464].
- [27] G. Jóhannesson, T.A. Porter and I.V. Moskalenko, *The Three-dimensional Spatial Distribution of Interstellar Gas in the Milky Way: Implications for Cosmic Rays and High-energy Gamma-ray Emissions*, *ApJ* **856** (2018) 45 [1802.08646].

- [28] T.A. Porter, G. Jóhannesson and I.V. Moskalenko, *High-energy Gamma Rays from the Milky Way: Three-dimensional Spatial Models for the Cosmic-Ray and Radiation Field Densities in the Interstellar Medium*, *ApJ* **846** (2017) 67 [1708.00816].
- [29] X.H. Sun, W. Reich, A. Waelkens and T.A. Enßlin, *Radio observational constraints on Galactic 3D-emission models*, *A&A* **477** (2008) 573 [0711.1572].
- [30] É. Jaupart, É. Parizot and D. Allard, *Contribution of the Galactic centre to the local cosmic-ray flux*, *A&A* **619** (2018) A12 [1808.02322].
- [31] R.C. Anjos and F. Catalani, *Galactic Center as an efficient source of cosmic rays*, *PRD* **101** (2020) 123015 [2006.02584].
- [32] G. Jóhannesson, T.A. Porter and I.V. Moskalenko, *Cosmic-Ray Propagation in Light of the Recent Observation of Geminga*, *ApJ* **879** (2019) 91 [1903.05509].
- [33] D. Malyshev, I. Cholis and J. Gelfand, *Pulsars versus dark matter interpretation of ATIC/PAMELA*, *PRD* **80** (2009) 063005 [0903.1310].
- [34] H. Zeng, Y. Xin, S. Zhang and S. Liu, *TeV Cosmic-Ray Nucleus Acceleration in Shell-type Supernova Remnants with Hard  $\gamma$ -Ray Spectra*, *ApJ* **910** (2021) 78 [2102.03465].
- [35] H. Zeng, Y. Xin, S. Zhang and S. Liu, *TeV Cosmic-Ray Nucleus Acceleration in Shell-type Supernova Remnants with Hard  $\gamma$ -Ray Spectra*, *ApJ* **910** (2021) 78 [2102.03465].
- [36] G. Jóhannesson, T.A. Porter and I.V. Moskalenko, *The Three-dimensional Spatial Distribution of Interstellar Gas in the Milky Way: Implications for Cosmic Rays and High-energy Gamma-ray Emissions*, *ApJ* **856** (2018) 45 [1802.08646].
- [37] M. Araya, *Detection of gamma-ray emission in the region of the supernova remnants G296.5+10.0 and G166.0+4.3*, *MNRAS* **434** (2013) 2202 [1306.5619].
- [38] Cherenkov Telescope Array Consortium, B.S. Acharya, I. Agudo, I. Al Samarai, R. Alfaro, J. Alfaro et al., *Science with the Cherenkov Telescope Array* (2019), 10.1142/10986.
- [39] M. Aguilar, L. Ali Cavasonza, G. Ambrosi, L. Arruda, N. Attig, F. Barao et al., *The Alpha Magnetic Spectrometer (AMS) on the international space station: Part II - Results from the first seven years*, *Physics Reports* **894** (2021) 1.
- [40] T. Sanuki, M. Motoki, H. Matsumoto, E.S. Seo, J.Z. Wang, K. Abe et al., *Precise Measurement of Cosmic-Ray Proton and Helium Spectra with the BESS Spectrometer*, *ApJ* **545** (2000) 1135 [astro-ph/0002481].
- [41] C. Consolandi, *Precision Measurement of the Proton Flux in Primary Cosmic Rays from 1 GV to 1.8 TV with the Alpha Magnetic Spectrometer on the International Space Station*, *arXiv e-prints* (2016) arXiv:1612.08562 [1612.08562].
- [42] Q. An, R. Asfandiyarov, P. Azzarello, P. Bernardini, X.J. Bi, M.S. Cai et al., *Measurement of the cosmic ray proton spectrum from 40 GeV to 100 TeV with the DAMPE satellite*, *Science Advances* **5** (2019) eaax3793 [1909.12860].
- [43] Y.S. Yoon, T. Anderson, A. Barrau, N.B. Conklin, S. Coutu, L. Derome et al., *Proton and Helium Spectra from the CREAM-III Flight*, *ApJ* **839** (2017) 5 [1704.02512].
- [44] E. Atkin, V. Bulatov, V. Dorokhov, N. Gorbunov, S. Filippov, V. Grebenyuk et al., *New Universal Cosmic-Ray Knee near a Magnetic Rigidity of 10 TV with the NUCLEON Space Observatory*, *Soviet Journal of Experimental and Theoretical Physics Letters* **108** (2018) 5 [1805.07119].
- [45] A.D. Panov, J.H. Adams, H.S. Ahn, G.L. Bashinzhagyan, J.W. Watts, J.P. Wefel et al., *Energy spectra of abundant nuclei of primary cosmic rays from the data of ATIC-2 experiment: Final results*, *Bulletin of the Russian Academy of Sciences, Physics* **73** (2009) 564 [1101.3246].



- [46] F. Alemanno, Q. An, P. Azzarello, F.C.T. Barbato, P. Bernardini, X.J. Bi et al., *Measurement of the Cosmic Ray Helium Energy Spectrum from 70 GeV to 80 TeV with the DAMPE Space Mission*, *PRL* **126** (2021) 201102 [[2105.09073](#)].
- [47] M. Aguilar, D. Aisa, B. Alpat, A. Alvino, G. Ambrosi, K. Andeen et al., *Precision Measurement of the Helium Flux in Primary Cosmic Rays of Rigidities 1.9 GV to 3 TV with the Alpha Magnetic Spectrometer on the International Space Station*, *PRL* **115** (2015) 211101.
- [48] M. Aguilar, L. Ali Cavasonza, B. Alpat, G. Ambrosi, L. Arruda, N. Attig et al., *Precision Measurement of Cosmic-Ray Nitrogen and its Primary and Secondary Components with the Alpha Magnetic Spectrometer on the International Space Station*, *PRL* **121** (2018) 051103.
- [49] M. Aguilar, L.A. Cavasonza, M.S. Allen, B. Alpat, G. Ambrosi, L. Arruda et al., *Properties of Iron Primary Cosmic Rays: Results from the Alpha Magnetic Spectrometer*, *PRL* **126** (2021) 041104.
- [50] O. Adriani, Y. Akaike, K. Asano, Y. Asaoka, M.G. Bagliesi, E. Berti et al., *Direct Measurement of the Cosmic-Ray Carbon and Oxygen Spectra from 10 GeV/n to 2.2 TeV/n with the Calorimetric Electron Telescope on the International Space Station*, *PRL* **125** (2020) 251102 [[2012.10319](#)].
- [51] O. Adriani, G.C. Barbarino, G.A. Bazilevskaya, R. Bellotti, M. Boezio, E.A. Bogomolov et al., *Measurement of Boron and Carbon Fluxes in Cosmic Rays with the PAMELA Experiment*, *ApJ* **791** (2014) 93 [[1407.1657](#)].
- [52] O. Adriani, Y. Akaike, K. Asano, Y. Asaoka, E. Berti, G. Bigongiari et al., *Cosmic-Ray Boron Flux Measured from 8.4 GeV/n to 3.8 TeV/n with the Calorimetric Electron Telescope on the International Space Station*, *PRL* **129** (2022) 251103 [[2212.07873](#)].

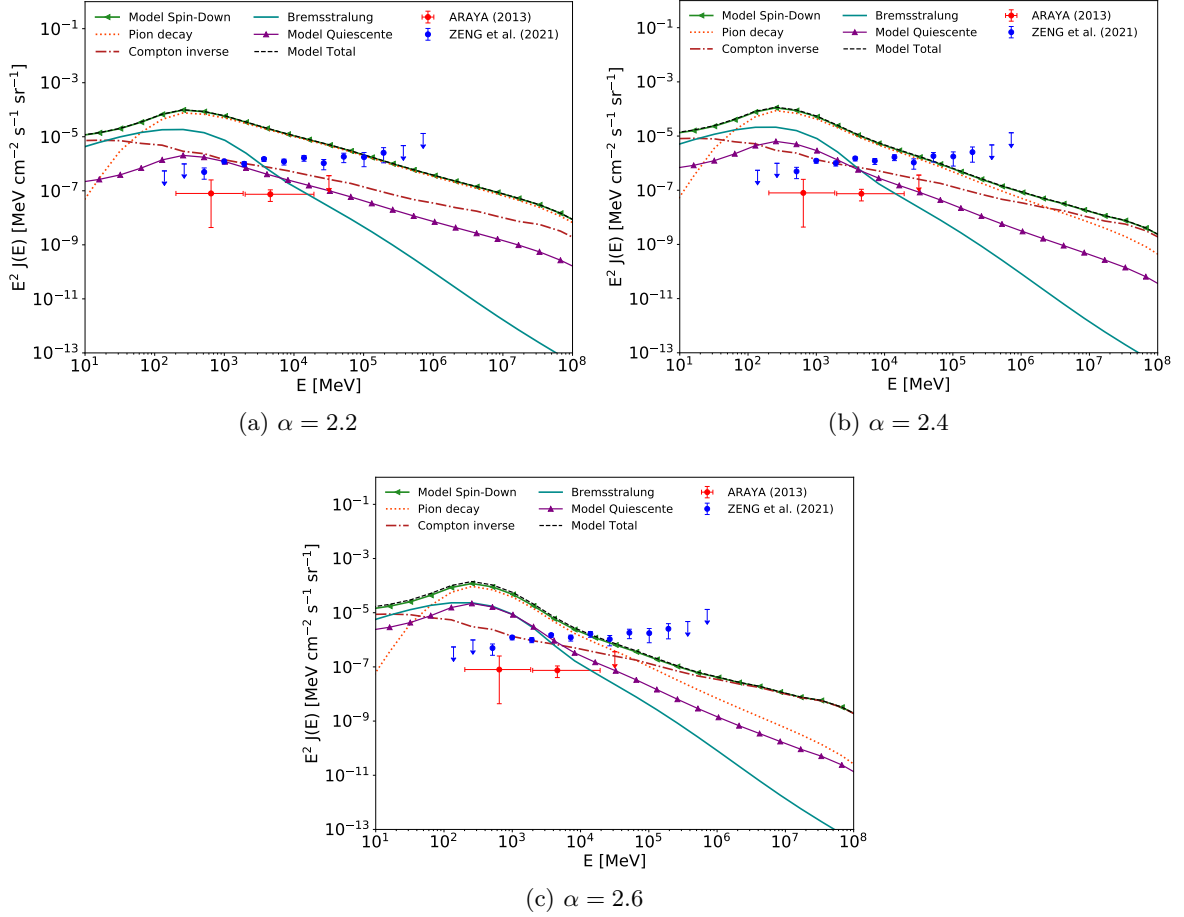


**Figure 1:** Spectral Energy Distribution of gamma-ray emissions resulting from cosmic rays in CCO 1E 1207.4-5209 and its associated Supernova Remnant (SNR) G296.5 + 10.0. The model spin-down includes contributions from pion decay, inverse Compton scattering, and bremsstrahlung. The total power injected by the source (Model Total) is denoted as the model sum. The data points featured in the plots are derived from the model developed by Zeng et al. in 2021 [35] and from gamma-ray measurements conducted by Araya in 2013 [37], focusing on the CCO+SNR association. See text for details. These models utilize a 2D gas distribution as described by Johannesson in 2018 [36].

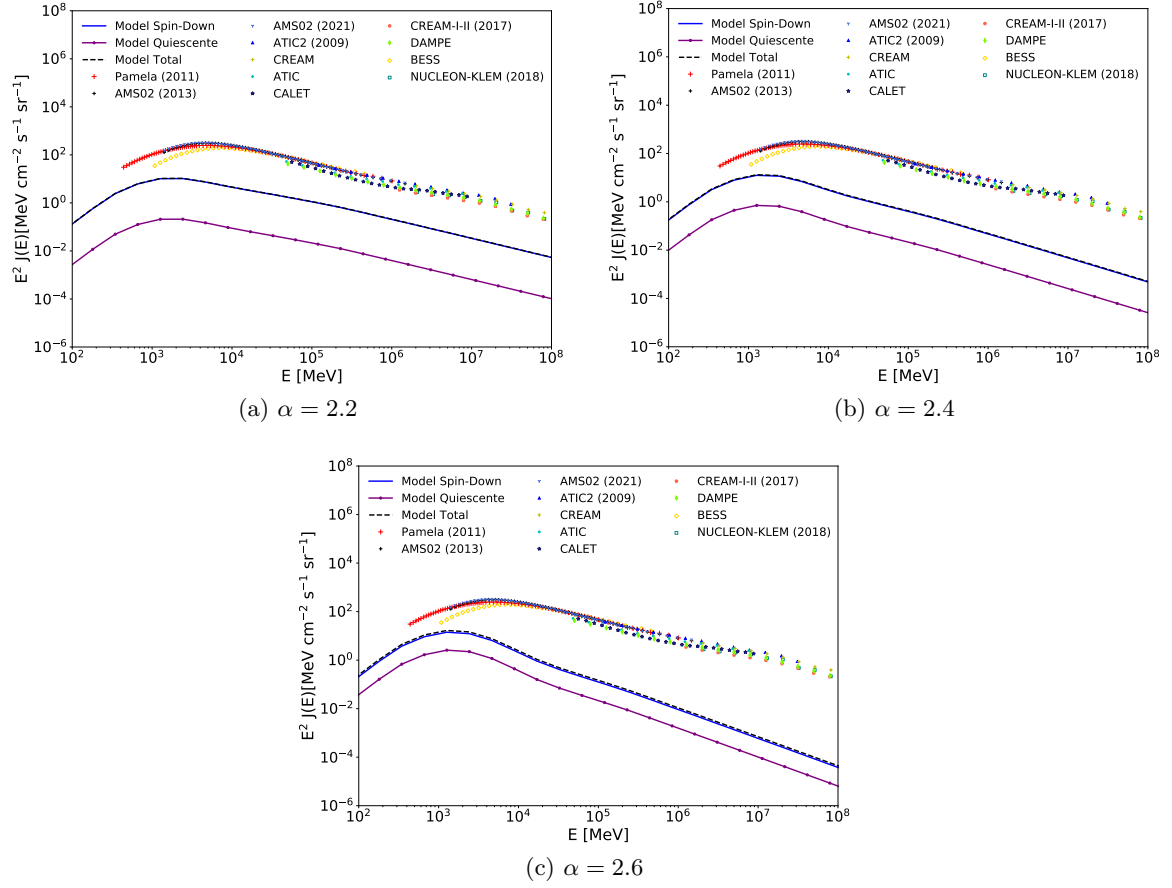


**Figure 2:** Energy spectra for proton. The spectra are multiplied by  $E^2$ . The models calculations are shown in comparison with the data considering a modulation of 0.30 GV. The data have been extracted from [39–45].

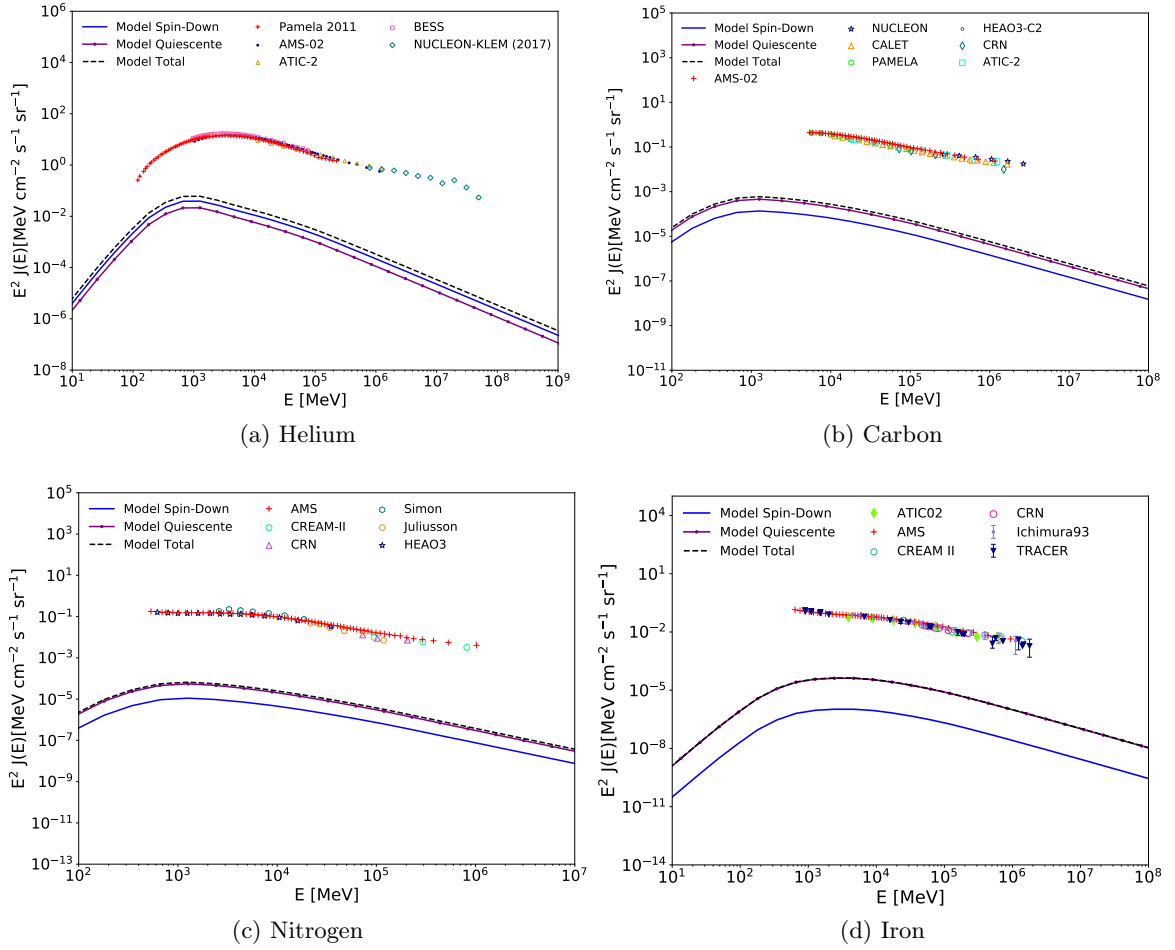


**Figure 3:** Energy spectra for four elements: helium, carbon, nitrogen and iron. The spectra are multiplied by  $E^2$ . The models calculations are shown in comparison with the data considering spectral index of 2.4 and a modulation of 0.30 GV. The data have been extracted [46–50].

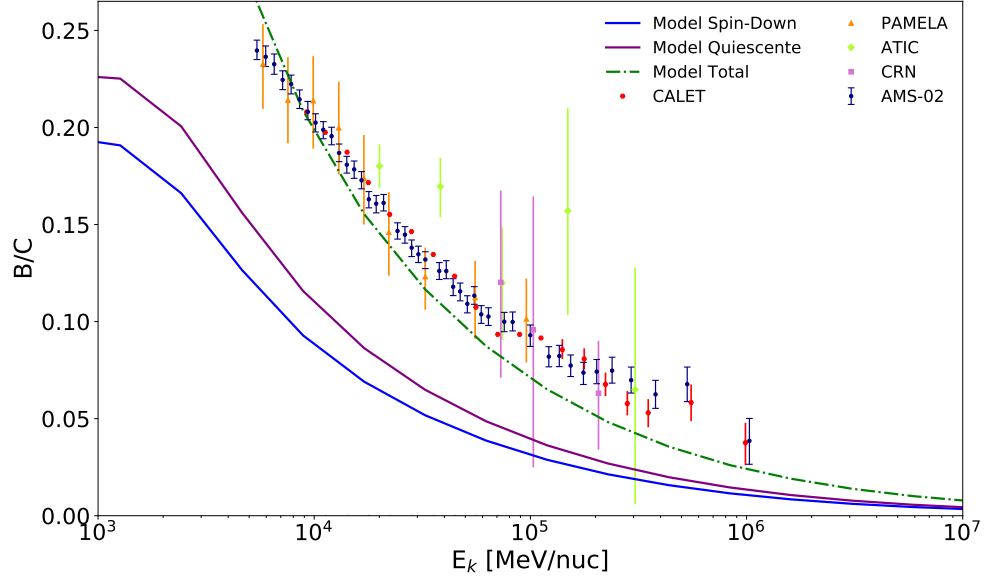


**Figure 4:**  $B/C$  ratio as function of kinetic energy per nucleon for the simulation models are shown in comparison with data from [51, 52].

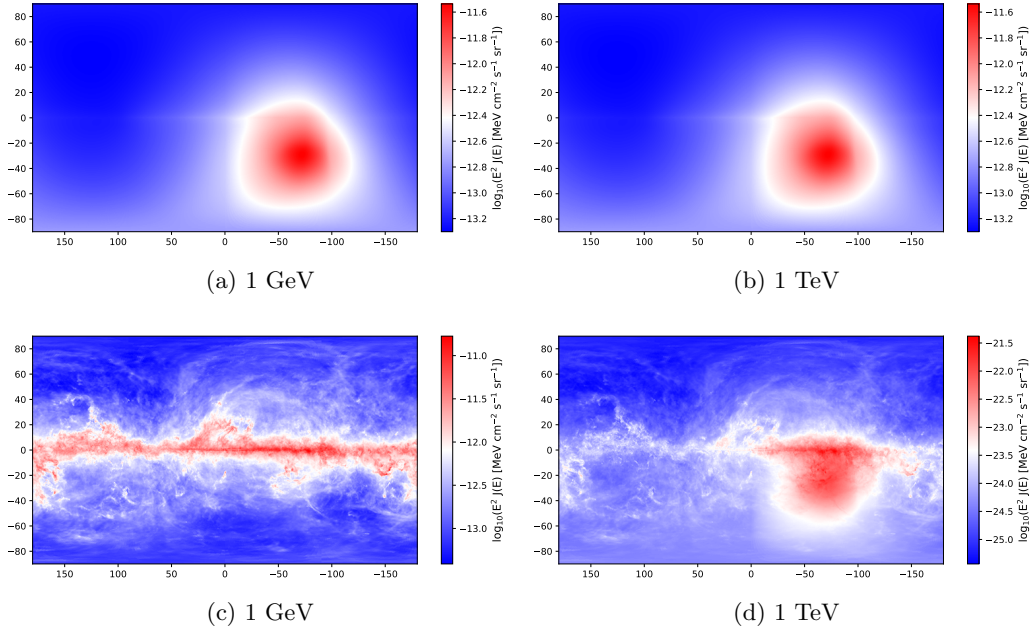


**Figure 5:** Gamma ray intensity at 1 GeV and 1 TeV from CCO 1E 1207.4-5209 and its host star SNR G296.5 + 10.0 for the spin-down model. The maps show the production of gamma rays by inverse Compton scattering - (a,b) and bremsstrahlung - (c,d). The maps are in Galactic coordinates with (1, b) = (0, 0) at the center of the map.